Available online at www.sciencedirect.com

SciVerse ScienceDirect

Procedia Technology 1 (2012) 496 – 504

Procedia Technology

INSODE 2011

# Effect of Thickness Variation on the Mechanical Buckling Load in Plates Made of Functionally Graded Materials

Hamid Mozafari[a*], Amran Ayob[a]

[a] Faculty of Mechanical Engineering, Universiti Teknologi Malaysia, 81310 UTM Skudai, Johor, Malaysia

**Abstract**

In this paper, the mechanical buckling load on a simply supported plate made of Functionally Graded Materials (FGM) with linearly varying thickness is considered. The material properties are assumed to vary as a power law though the plate thickness. Based on higher–order theory assumptions, the equilibrium, stability equations and the relations for pre-buckling loads of the plate under mechanical load are obtained by using a variational formulation. The equations are based on Love-Kirchhoff hypothesis and the Sanders non-liner strain-displacement relations. The closed form solution for the buckling load is obtained and the result is verified against known case i.e. a plate with constant thickness. The buckling load is derived by employing the weighted residual approach. Finally, different plots indicating the variation of buckling load vs. different FGM materials, geometries and loading conditions were obtained.

*Keywords:* Buckling load, FGM plate; Thin plate, Higher-order theory, Plate with variable thickness

## 1. Introduction

Buckling of plates is in most cases an undesirable and harmful phenomenon. Therefore, by accurate calculations and necessary predictions in design, bending must be avoided. It is possible through a complete understanding of the mechanical behaviour, the boundary conditions, and the type of the Functionally Graded Materials (FGM).Such Functionally Graded Materials are composite materials (e.g. metal and ceramic) with varying properties through the thickness. They have thermo-mechanical properties which vary through their thickness and were first conceived by a group of researchers in Japan [23].The main advantage of such materials is the possibility of tailoring the desired properties. Obviously, FGM's can be used in a variety of applications which have made them very attractive. For plate stability, the influence of critical buckling load is most important in design. The computed buckling load depends upon the criterion used to define buckled state of the plate.

Theories of plates and shells have already been applied to high extent, and there are many text books available, such as [1- 3]. Later on, the concept of FGM was proposed in [4] and [5].

The main advantage of Functionally Graded Materials is their high resistance to environments with extremely high temperature and extreme changes in temperature. Ceramic due to low thermal conductance constituents causes resistance to high temperature. One of the main functions of Functionally Graded Materials is the use in power reactors, electronic and magnetic sensors, medical engineering of artificial bones and teeth, chemical industry and all new technologies such as ceramic engines and (as) resistant covers and protection against corrosion.

Chi and Chung [9, 10] examined the mechanical behavior of FGM plates under transverse load. Najafizadeh and Eslami [14] studied the buckling behavior of circular FGM plates under uniform radial compression. Shariat and

* Hamid Mozafari.
*E-mail address*: Mozafari.h@gmail.com.


doi:10.1016/j.protcy.2012.02.108

Eslami [16] investigated thermal buckling of imperfect FGM plates. Huang and Chang [13] carried out studies on corner stress singularities in an FGM thin plate. Nonlinear analysis, such as nonlinear bending, nonlinear vibration and post-bucking analysis of homogeneous isotropic or FGM plates and shells can be found in the articles by Sundararajan et al. [17], Chen et al. [7], Hsieh and Lee [12] and Ghannad Pour and Alinia [11]. Further research can be found in the articles by Navazi et al. [15], Woo et al. [18], Chen and Tan [8] and Li et al. [20].Morimoto et al. [19] and Abrate [6] noticed that there is no stretching–bending coupling in constitutive equations if the reference surface is properly selected. Classical nonlinear laminated plate theory and the concept of physical neutral surface are employed to formulate the basic equations of the FGM thin plate. Da-Guang Zhanga and You-He Zhou studied functionally graded materials as thin plates in 2008[27], whereas Wu [21] has examined the effect of shear deformation on the thermal buckling of FGM plates. Chen and Liew [22] have examined the buckling of FGM plates subjected to in-plane edge loads. Salonitis and Pandremenos [27] have investigated the multi-phase and multi-functional material which is considered the various multifunctional materials reported in the literature and the processing means developed.

The above results show that critical temperature differences for the functionally graded plates are generally lower than the corresponding values for homogeneous plates. They used classical plate theory for the buckling analysis of functionally graded plates under in–plane compressive loading.

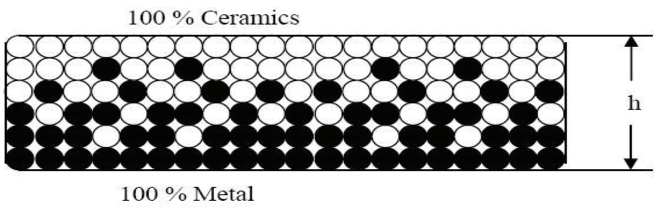


Figure 1: Schematic of a FGM across the plate thickness

A functionally graded plate made of a mixture of metal and ceramic is considered. The material properties are gradually varied from bottom surface pure metal to top surface pure ceramic where can be shown a section of the plate in Figure 1.

In the present article, equilibrium and stability equations for the functionally graded plates are obtained on the basis of higher order shear deformation plate theory. Resulting equations are employed to obtain the closed–form solutions for the critical buckling loads. In order to establish the fundamental system of equations for the buckling analysis, it is assumed that the non-homogeneous mechanical properties are given by a power form of the special coordinates.

## 2. Functionally Graded Material Plates

Functionally graded materials (FGMs) are typically made from a mixture of ceramics and a metal or a combination of different metals. The ceramic constituent of the material provides the high temperature resistance due to its low thermal conductivity. The ductile metal constituent, on the other hand, prevents fracture caused by thermal-stresses due to high temperature gradient in a very short period of time. Furthermore, a mixture of a ceramic and a metal with a continuously varying volume fraction can be easily manufactured [24, 25].

The volume fractions of the ceramic $V_c$ and metal $V_m$, $V_m + V_c = 1$ are assumed to follow a power law and are expressed as:

$$V_c(z) = \left(\frac{2z+h}{2h}\right)^k. \tag{1}$$

$z$ is the thickness coordinate ( $-h/2 \le z \le h/2$ ), $h$ is the thickness of the plate and $k$ is the power law index which takes values greater than or equal to zero. The variation of the composition of ceramics and metal is linear for $k$ =1. The value of $k$ equal to zero represents a pure ceramic plate. The mechanical and thermal properties of FGMs are determined from the volume fraction of the material constituents. We assume that the non-homogenous material properties such as the modulus of elasticity $E$ change in the thickness direction $z$ based on the Voigt's rule over the whole range of the volume fraction, while Poisson's ratio $\nu$ is assumed to be constant as:

$$E(z) = E_c V_c + E_{cm}(1 - V_c),$$
$$\alpha(z) = \alpha_c V_c + \alpha_{cm}(1 - V_c), \quad (2)$$
$$\upsilon(z) = \upsilon_0,$$

where subscripts m, c refer to the metal and ceramic constituents, respectively. By substituting Eqs. (1) into Eqs. (2), material properties of the FGM plate are determined, which are the same form as the equations proposed by Praveen and Reddy [26]:

$$\alpha(z) = \alpha_{\mathrm{m}} + \alpha_{\mathrm{cm}}\left(\frac{2z+h}{2h}\right)^k$$

and (3)

$$\upsilon(z) = \upsilon_0$$

where

$$E_{\mathrm{cm}} = E_{\mathrm{c}} - E_{\mathrm{m}} \text{ and } \alpha_{\mathrm{cm}} = \alpha_{\mathrm{c}} - \alpha_{\mathrm{m}}. \quad (4)$$

## 3. Buckling Analysis

Imperialist Consider a plate made of functionally graded material with simply supported edge conditions and subjected to an in-plane loading in two directions, as shown in Fig. 2. To obtain the critical buckling loads $F_x$ and $F_y$, the pre buckling forces should be found. Solving the membrane form of equilibrium equations, results in the following force resultants.

$$N_{x_0} = -\frac{p_x}{b}, \quad N_{x_0} = -\frac{p_x}{b}, \quad N_{y_0} = -\frac{p_y}{a}, N_{xy_0} = 0. \quad (5)$$

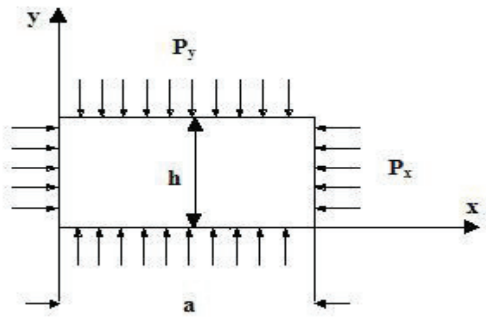


Figure 2: Plate subjected to in plane loading.

Equations (5) have two independent load parameters $\frac{F_x}{b}$ and $\frac{F_y}{a}$. Pre-buckling forces can be expressed by a single-parameter simply by letting,

$$\frac{F_y}{a} = R\frac{F_x}{b}, \quad (6)$$

where $R$ is a non-dimensional constant. The resulting equation then may be solved for a series of selected values of $R$. The simply supported boundary conditions are defined as,

$$w_0(x,0) = w_0(x,b) = w_0(0,y) = w_0(a,y) = 0,$$

$$p_y(x,0) = p_y(x,b) = p_x(0,y) = p_x(a,y) = 0,$$
$$M_y(x,0) = M_y(x,b) = M_x(0,y) = M_x(a,y) = 0,$$
$$u_0^1(x,0) = u_0^1(x,b) = v_0^1(0,y) = v_0^1(a,y) = 0, \quad (7)$$
$$v_1^1(x,0) = u_1^1(x,b) = v_1^1(0,y) = v_1^1(a,y) = 0.$$

The following approximate solutions are seen to satisfy both the differential equations and the boundary conditions

$$u_0^1 = u_{0mn} \cos\frac{m\pi}{a} x \sin\frac{n\pi y}{b},$$
$$u_1^1 = u_{1mn} \cos\frac{m\pi}{a} x \sin\frac{n\pi y}{b}, \quad (8)$$
$$v_0^1 = v_{0mn} \sin\frac{m\pi}{a} x \cos\frac{n\pi y}{b}, \qquad m, n = 1, 2, 3, ...$$
$$v_1^1 = v_{1mn} \sin\frac{m\pi}{a} x \cos\frac{n\pi}{b} y,$$
$$w_0^1 = w_{0mn} \sin\frac{m\pi}{a} x \sin\frac{n\pi y}{b} y.$$

where *m* and *n* are numbers of half waves in *x*- and *y*-directions, respectively, and $(u_{0mn}, u_{1mn}, \upsilon_{0mn}, \upsilon_{1mn}, \omega_{0mn})$ are constant coefficients. Substituting Eqs. (8) into the stability equations and using the kinematic and constitutive relations, yields a system of five homogeneous equations for $u_{0mn}, u_{1mn}, \upsilon_{0mn}, \upsilon_{1mn}$, and $\omega_{0mn,}$ i. e.

$$[k_{ij}] \begin{pmatrix} u_{0mn} \\ v_{0mn} \\ w_{0mn} \\ u_{1mn} \\ v_{1mn} \end{pmatrix} = 0, \quad (9)$$

In which $K_{ij}$ is a symmetric matrix with the components as follows:

$$k_{11} = E_1[(\frac{m\pi}{a})^2 + \frac{1-\upsilon_0}{2}(\frac{n\pi}{b})^2],$$
$$k_{12} = E_1 \frac{(1+\upsilon_0)}{2}(\frac{m\pi}{a})(\frac{n\pi}{b}),$$
$$k_{14} = (E_2 - \frac{4E_4}{3h^2})[(\frac{m\pi}{a})^2 + \frac{1-\upsilon_0}{2}(\frac{n\pi}{b})^2],$$
$$k_{15} = (\frac{E_2}{2} - \frac{2E_4}{3h^2})(1+\upsilon_0)(\frac{m\pi}{a})(\frac{n\pi}{b}),$$
$$k_{21} = k_{12},$$
$$k_{22} = E_1[\frac{1-\upsilon_0}{2}(\frac{m\pi}{a})^2 + (\frac{n\pi}{b})^2],$$
$$k_{23} = -\frac{4E_4}{3h^2}[((\frac{m\pi}{a})^2(\frac{n\pi}{b}) + (\frac{n\pi}{b})^3],$$

$$
\begin{aligned}
&k_{24} = (\frac{E_2}{2} - \frac{2E_4}{3h^2})(1+\upsilon_0)(\frac{m\pi}{a})(\frac{n\pi}{b}),\\
&k_{25} = (2 - \frac{4E_4}{3h^2})[\frac{1-\upsilon_0}{2}(\frac{m\pi}{a})^2 + (\frac{n\pi}{b})^2],\\
&k_{31} = k_{13},\\
&k_{32} = k_{23},\\
&\bar{k}_{33} = \frac{16E_7}{9h^4}[(\frac{m\pi}{a})^2 + (\frac{n\pi}{b})^2]^2 - (\frac{4E_3}{h^2} - \frac{E_1}{2} - \frac{8E_5}{h^2})\\
&.(1-\upsilon_0)[(\frac{m\pi}{a})^2 + (\frac{n\pi}{b})^2] + (1-\upsilon_0^2)]N_{x_0}(\frac{m\pi}{a})^2 + N_{y_0}(\frac{n\pi}{b})^2],\\
&k_{34} = -(\frac{4E_3}{h^2} - \frac{E_1}{2} - \frac{8E_5}{h^4})(1-\upsilon_0)(\frac{m\pi}{a}) + (\frac{16E_7}{9h^4} - \frac{4E_5}{3h^2})[(\frac{m\pi}{a})^3 + (\frac{m\pi}{a})(\frac{n\pi}{b})^2],\\
&k_{35} = -(\frac{4E_3}{h^2} - \frac{E_1}{2} - \frac{8E_5}{h^4})(1-\upsilon_0)(\frac{n\pi}{b}) + (\frac{16E_7}{9h^4} - \frac{4E_5}{3h^2})[(\frac{m\pi}{a})^2(\frac{m\pi}{b}) + (\frac{n\pi}{b})^3],\\
&k_{41} = -k_{14},\\
&k_{42} = -k_{24},\\
&k_{43} = -k_{34},\\
&k_{44} = (\frac{8E_5}{3h^2} - \frac{16E_7}{9h^4} - E_3)[(\frac{m\pi}{a})^2 + \frac{1-\upsilon_0}{2}(\frac{n\pi}{b})^2] - (\frac{E_1}{2} - \frac{4E_3}{h^2} + \frac{8E_5}{h^4})(1-\upsilon_0),\\
&k_{45} = (\frac{4E_5}{3h^2} - \frac{E_3}{2} - \frac{8E_7}{9h^2}E_3)(\frac{m\pi}{a})(\frac{n\pi}{b}),\\
&k_{51} = -k_{15},\\
&k_{52} = -k_{25},\\
&k_{53} = -k_{35},\\
&k_{54} = k_{45},\\
&k_{55} = (\frac{8E_5}{3h^2} - \frac{16E_7}{9h^4} - E_3)[\frac{1-\upsilon_0}{2}(\frac{m\pi}{a})^2 + (\frac{n\pi}{b})^2](\frac{E_1}{2} - \frac{4E_3}{h} + \frac{8E_5}{h^4})(1-\upsilon_0).
\end{aligned}
\tag{10}
$$

Substituting pre-bucking forces from Eqs. (5) and (6) into the relation of $K_{33}$ and setting $|K_{ij}| = 0$ to obtain the nonzero solution, the value of the $F_x$ is found as:

$$
p_x = \frac{b^3 k_d}{\pi^2(1-\upsilon_0^2)k_c[(\frac{mb}{a})^2 + Rn^2]}, \tag{11}
$$

where

$$
\begin{aligned}
&k_3 = k_{15}k_{24}k_{42}k_{51} + k_{12}k_{25}k_{22}k_{51} + k_{14}k_{22}k_{45}k_{51} +\\
&k_{14}k_{25}k_{41}k_{52} + k_{15}k_{21}k_{44}k_{52} + k_{11}k_{24}k_{45}k_{52} +\\
&k_{15}k_{22}k_{41}k_{54} + k_{11}k_{25}k_{42}k_{54} + k_{12}k_{21}k_{45}k_{54} +\\
&k_{12}k_{24}k_{41}k_{55} + k_{14}k_{21}k_{42}k_{55} + k_{11}k_{22}k_{44}k_{55} -\\
&k_{14}k_{25}k_{42}k_{51} - k_{15}k_{22}k_{44}k_{51} - k_{12}k_{24}k_{45}k_{51} -\\
&k_{15}k_{24}k_{41}k_{52} - k_{11}k_{25}k_{44}k_{52} - k_{14}k_{21}k_{45}k_{52} -\\
&k_{12}k_{25}k_{41}k_{54} - k_{15}k_{21}k_{42}k_{54} - k_{11}k_{22}k_{45}k_{54} -\\
&k_{14}k_{22}k_{41}k_{55} - k_{11}k_{24}k_{42}k_{55} - k_{12}k_{21}k_{44}k_{55},
\end{aligned}
\tag{12}
$$

and

$k_d = \mathrm{Det}[k_{ij}]$ i, j = 1, 2, 3…

The value of the deviation is found as

$$\Delta = \left( \frac{P_C - P_T}{P_T} \right) * 100. \tag{13}$$

The critical buckling load $F_{xc}$ is obtained for the values of *m* and *n* that make the preceding expression a minimum. The plate is subjected to the biaxial compression, when *R* is selected to be positive. The plate is subjected to the uniaxial compression along the *x* axis, when *R* is equal to zero. Negative values of *R* signify tensile loading in the *y*-direction while the plate is under compression along the *x*-direction. As would be expected on intuitive grounds, the addition of a tensile load in the transverse direction is seen to have a stabilizing influence. By setting the power law index equal to one (*k*=1), Eq. (11) is reduced to the critical load for a functionally graded plate with linear composition of ceramics and metal. Also, by setting the power law index equal to zero (*k* = 0), Eq. (11) is reduced to the critical load of homogeneous plates.

## 4. Numerical Example and Discussions

To illustrate the proposed approach, a ceramic-metal functionally graded plate is considered. The combination of materials consists of aluminium and alumina. The Young's modulus for aluminium is $E_m$ = 70 GPa and for alumina is $E_c$ = 380 GPa, respectively. The Poisson's ratio is chosen to be 0.3 for both. The plate is assumed to be simply supported on all four edges.

Variation of the critical buckling load $F_{xc}$ versus the aspect ratio *b/a*, side to thickness ratio *b/h*, and power law index *k* are inserted for three loading cases in Table |1| through Table |3|. In each table, the values of critical buckling load $F_{xc}$ obtained by the method developed in the present article based on the higher-order theory are compared to their respective values obtained from the classical plate theory. Also, the tables are shown the first order shear deformation (F) theory.

In Tables |1| the results of the buckling analysis for the plate under biaxial compression (*R*=1) are presented. Table |1| shows that the buckling load increases by the increase of the aspect ratio *b/a,* and decreases by the increase of the power law index (*k*) from zero to 10.

The critical buckling loads obtained based on the higher-order plate theory are noticeably greater than values obtained based on the higher-order shear deformation theory. The differences are considerable for long thin plates where for example an improvement of 12% can be absented (*k* = 10, *b/a* = 10).

In Tables |2| the results of the buckling analysis for the plate under uniaxial compression (*R*=0) are presented. It is concluded that similar to the previous loading case, the buckling load increases by the increase of the aspect ratio *b/a*, decreases by the increase of the power law index (*k*), and decreases by the increase of the dimension ratio *b/h*. Also, the critical buckling loads obtained based on the higher-order plate theory are noticeably greater than the values obtained based on higher order shear deformation theory. The differences are considerable for long and thin plate, e.g.10% improvement for*k* = 10, *b/a* = 10.

In Tables |3| the results of the buckling analysis for the plate under compression along the *x*-direction and tension along the *y*-direction (*R*=-1) are presented. The trend is similar to the previous loading cases. Comparing Tables |1| with Table |2| show that the critical buckling loads for the plate under uniaxial compression are greater than the plate under biaxial compression. This conclusion can be obtained when analysis is based on classical or higher-order theory. It is understood that the third order shear deformation (T) is much closer to the first order shear deformation (F) theory in comparison with the classical plate theory.

Table 1: Critical buckling loads [kN] of the FG plate under biaxial compression due to the classical (C), Third order (T) and First order (F) theories respect to *k* and *b/a*

| k | | *b/a*=1 | *b/a*=2 | *b/a*=3 | *b/a*=4 | *b/a*=5 | b/a = 6 | b/a = 7 | b/a = 8 | b/a = 9 | b/a = 10 |
|---|---|---|---|---|---|---|---|---|---|---|---|
| C | | 171.724 | 429.310 | 858.619 | 1459.653 | 2232.411 | 3179.012 | 4300.455 | 5596.121 | 7069.644 | 8542.665 |
| Δ | *K*=0 | 1.12 | 1.53 | 1.91 | 2.44 | 2.94 | 3.61 | 4.82 | 6.12 | 7.38 | 8.42 |
| T | | 169.822 | 422.840 | 842.527 | 1424.886 | 2168.653 | 3068.248 | 4102.705 | 5273.39 | 6583.762 | 7879.234 |
| F | | 170.012 | 423.754 | 8.44.322 | 1427.256 | 2173.120 | 3075.560 | 4135.251 | 5298.012 | 6645.205 | 7922.653 |

| | | | | | | | | | | | |
|---|---|---|---|---|---|---|---|---|---|---|---|
| **C** | | 85.594 | 213.985 | 427.971 | 727.550 | 1112.724 | 1584.118 | 2143.067 | 2790.443 | 3525.667 | 4349.098 |
| Δ | *K*=1 | 1.31 | 1.81 | 2.43 | 3.36 | 4.11 | 5.29 | 6.28 | 7.42 | 8.51 | 9.62 |
| **T** | | 84.487 | 210.181 | 417.818 | 703.899 | 1068.796 | 1504.528 | 2016.435 | 2597.694 | 3249.163 | 3967.431 |
| **F** | | 84.721 | 210.904 | 419.214 | 707.260 | 1074.023 | 1516.625 | 2042.290 | 2635.450 | 3301.211 | 4001.252 |
| **C** | | 56.483 | 141.208 | 282.415 | 480.106 | 734.280 | 1045.097 | 1414.665 | 1841.006 | 2327.766 | 2872.889 |
| Δ | *K*=5 | 1.42 | 1.91 | 2.6 | 3.55 | 4.43 | 5.67 | 6.83 | 7.92 | 9.11 | 10.32 |
| **T** | | 55.692 | 138.561 | 275.258 | 463.646 | 703.131 | 989.019 | 1324.221 | 1705.899 | 2133.412 | 2604.142 |
| **F** | | 55.801 | 138.905 | 276.980 | 467.036 | 708.551 | 1004.255 | 1332.514 | 1738.252 | 2149.208 | 2651.840 |
| **C** | | 51.443 | 128.620 | 257.240 | 437.307 | 668.823 | 951.332 | 1287.445 | 1676.776 | 2119.006 | 2616.546 |
| Δ | *K*=10 | 1.81 | 2.33 | 3.41 | 4.63 | 5.9 | 7.12 | 8.34 | 9.52 | 10.85 | 12.13 |
| **T** | | 50.528 | 125.691 | 248.757 | 417.956 | 631.561 | 889.099 | 1188.338 | 1531.023 | 1911.598 | 2333.493 |
| **F** | | 50.615 | 125.918 | 249.812 | 420.233 | 637.124 | 904.362 | 1195.180 | 1549.541 | 1932.530 | 2394.320 |

Comparing Table |2| with Tables |3| show that the critical buckling loads for the plate under compression along the *x*-direction and tension along the *y*-direction are greater than the plate under uniaxial compression. This conclusion can be obtained when the analysis is based on the classical or higher order theory. Although the results of the first order and the third order theories are close to each other, it is recommended that one uses the third order shear deformation theory for thin plates.

Table 2: Critical buckling loads [kN] of the FG plate under uniaxial compression due to the classical (C), Third order (T) and First order (F) theories respect to *k* and *b/a*

| **k** | | ***b/a*=1** | ***b/a*=2** | ***b/a*=3** | ***b/a*=4** | ***b/a*=5** | **b/a = 6** | **b/a = 7** | **b/a = 8** | **b/a = 9** | **b/a = 10** |
|---|---|---|---|---|---|---|---|---|---|---|---|
| **C** | | 343.448 | 536.637 | 954.022 | 1550.881 | 2321.707 | 3265.480 | 4380.908 | 5664.434 | 7115.009 | 8730.098 |
| Δ | *K*=0 | 0.91 | 1.33 | 1.71 | 2.23 | 2.74 | 3.44 | 4.58 | 5.89 | 7.26 | 8.6 |
| **T** | | 340.351 | 529.593 | 937.982 | 1517.051 | 2259.789 | 3156.883 | 4189.05 | 5349.357 | 6633.423 | 8038.764 |
| **F** | | 340.802 | 530.255 | 939.411 | 1519.512 | 2264.110 | 3163.402 | 4197.512 | 5358.212 | 6652.02 | 8097.810 |
| **C** | | 171.188 | 267.482 | 475.523 | 773.022 | 1157.233 | 1625.776 | 2176.878 | 2810.990 | 3526.554 | 4323.767 |
| Δ | *K*=1 | 1.13 | 1.52 | 1.91 | 2.56 | 2.87 | 3.73 | 4.91 | 6.28 | 7.66 | 9.01 |
| **T** | | 169.275 | 263.477 | 466.611 | 753.727 | 1124.947 | 1567.315 | 2074.996 | 2644.891 | 3275.64 | 3966.395 |
| **F** | | 169.612 | 263.905 | 468.103 | 756.302 | 1129.08 | 1574.520 | 2086.09 | 2654.052 | 3292.921 | 4005.692 |
| **C** | | 112.966 | 176.510 | 313.795 | 510.113 | 763.651 | 1068.667 | 1423.354 | 1827.099 | 2279.903 | 2778.213 |
| Δ | *K*=5 | 1.37 | 1.83 | 2.34 | 3.43 | 4.22 | 5.12 | 6.28 | 7.35 | 8.54 | 9.98 |
| **T** | | 111.439 | 173.338 | 306.62 | 493.196 | 732.73 | 1016.616 | 1339.249 | 1702.002 | 2100.519 | 2526.519 |
| **F** | | 111.712 | 173.872 | 308.077 | 496.214 | 738.581 | 1025.62 | 1350.119 | 1716.310 | 2121.150 | 2560.260 |
| **C** | | 102.896 | 160.775 | 285.822 | 464.639 | 695.576 | 977.065 | 1309.566 | 1690.445 | 2118.221 | 2592.908 |
| Δ | *K*=10 | 1.64 | 2.19 | 2.84 | 3.70 | 4.81 | 5.43 | 6.78 | 7.94 | 9.37 | 10.92 |
| **T** | | 101.236 | 157.329 | 277.929 | 448.061 | 663.654 | 926.743 | 1226.415 | 1566.097 | 1936.748 | 2337.638 |
| **F** | | 101.425 | 157.891 | 279.140 | 451.210 | 669.109 | 933.890 | 1237.362 | 1581.360 | 1958.812 | 2382.039 |

Table 3: Critical buckling loads [kN] of the FG plate under combined compression and tension due to the classical (C), Third order (T) and First order (F) theories respect to *k* and *b/a*

| **k** | | ***b/a*=1** | ***b/a*=2** | ***b/a*=3** | ***b/a*=4** | ***b/a*=5** | **b/a = 6** | **b/a = 7** | **b/a = 8** | **b/a = 9** | **b/a = 10** |
|---|---|---|---|---|---|---|---|---|---|---|---|
| **C** | | 715.516 | 715.516 | 1073.274 | 1654.273 | 2418.445 | 3343.778 | 4414.321 | 5621.091 | 6959.002 | 8426.664 |
| Δ | *K*=0 | 1.23 | 1.23 | 1.81 | 2.64 | 3.52 | 4.66 | 5.83 | 7.12 | 8.51 | 9.62 |
| **T** | | 706.822 | 706.822 | 1054.193 | 1611.723 | 2336.21 | 3194.896 | 4171.143 | 5247.471 | 6413.236 | 7687.159 |
| **F** | | 707.315 | 707.315 | 1056.290 | 1615.065 | 2342.612 | 3205.113 | 4185.367 | 5268.210 | 6448.312 | 7740.26 |
| **C** | | 356.642 | 356.642 | 534.308 | 824.557 | 1205.451 | 1667.334 | 2206.115 | 2820.712 | 3507.122 | 4266.355 |
| Δ | *K*=1 | 1.31 | 1.31 | 1.93 | 2.72 | 3.74 | 4.82 | 6.01 | 7.32 | 8.81 | 10.12 |
| **T** | | 352.030 | 352.030 | 524.191 | 802.723 | 1161.992 | 1590.664 | 2081.044 | 2628.319 | 3223.161 | 3874.278 |
| **F** | | 353.815 | 353.815 | 526.261 | 806.945 | 1167.290 | 1601.854 | 2095.369 | 2647.351 | 3258.927 | 3923.549 |

| | | | | | | | | | | | |
|---|---|---|---|---|---|---|---|---|---|---|---|
| **C** | | 235.342 | 235.346 | 353.019 | 544.120 | 795.470 | 1097.077 | 1444.656 | 1832.903 | 2258.332 | 2721.546 |
| Δ | ***K*=5** | 1.52 | 1.52 | 2.14 | 2.93 | 4.07 | 5.12 | 6.33 | 7.63 | 9.12 | 10.73 |
| **T** | | 231.822 | 231.822 | 345.623 | 528.631 | 764.361 | 1043.643 | 1358.653 | 1702.967 | 2069.586 | 2457.822 |
| **F** | | 232.512 | 232.512 | 347.258 | 602.51 | 770.052 | 1054.263 | 1371.712 | 1723.104 | 2103.421 | 2505.579 |
| **C** | | 214.366 | 214.366 | 321.549 | 495.615 | 724.558 | 1002.012 | 1326.803 | 1693.006 | 2101.343 | 2553.533 |
| Δ | ***K*=10** | 1.94 | 1.94 | 2.42 | 3.12 | 4.15 | 5.36 | 6.88 | 8.81 | 11.13 | 12.51 |
| **T** | | 210.286 | 210.286 | 313.951 | 480.62 | 695.687 | 951.036 | 1241.395 | 1555.929 | 1890.887 | 2269.605 |
| **F** | | 211.023 | 211.023 | 315.481 | 484.592 | 670.562 | 962.510 | 1267.032 | 1576.213 | 1926.003 | 2318.915 |

## 5. Conclusion

In the presented paper, the derivations were based on the first and third-order shear deformation theory, with the assumption of power law composition for the constituent materials. Then, the buckling analyses of functionally graded (FG) plates under in-plane compression are presented. Closed form solutions for the critical buckling loads of plates are presented. The higher-order shear deformation theory underestimates the buckling load compared with the first and third order plate theory. The critical buckling load $F_{xc}$ for the FG plates is reduced when the power law index *k* increases. Also, the critical buckling load $F_{xc}$ for the FG plates increases with increasing the aspect ratio *b/a*.

## References


1. Brush DO, Almroth BO. *Bucking of Bars, Plates and Shells*, Second Ed., New York, McGraw-Hill, (1975).

2. Timoshenko S, Woinowsky-KriegerS. *Theory of plates and shells*, Second Ed., New York, Mc Graw-Hill, (1959).
3. Zheng XJ. *The theory and application for large deflection of Circular plate*, Ji-Lin Science Technology press. Chinese: Chang-Chun, (1990) 45-90.
4. Yamanouchi M, Koizumi M, Shiota I. Proceedings of the First International Symposium on Functionally Gradient Materials. Japan, (1990) 273-281.
5. Koizumi M. The concept of FGM, Ceram: Trans., Funct. Grad Mater. 34 (1993) 3-10.
6. Abrate S. Functionally graded material behave like homogeneous plates. Composites Part B: Engineering, 39(1) (2008) 151–158.
7. Chen CS, Chen TJ, Chien RD, Nonlinear vibration analysis of an initially stressed functionally graded plate, Thin-Walled Structures, 44(8) (2006) 844–851.
8. Chen CS, Tan AH. Imperfection sensitivity in the nonlinear vibration of initially stresses functionally graded plates, Composite Structures, 78(4) (2007) 529–536.
9. Chi SH, Chung YL. Mechanical behavior of functionally graded material under transverse load, International Journal of Solids and Structures, 43(13) (2006) 3657–3674.
10. Chi SH, Chung YL. Mechanical behavior of functionally graded material, International Journal of Solids and Structures, 43(13) (2006) 3675–3691.
11. Ghannadpour SAM, Alinia MM. Large deflection behavior of functionally graded plates under pressure loads, Composite Structures, 75(1–4) (2006) 67–71.
12. Hsieh JJ, Lee LT. An inverse problem for a functionally graded elliptical, International Journal of Solids and Structures, 43(20) (2006) 5981–5993.
13. Huang CS, Chang MJ. Corner stress singularities in an FGM thin plate, International Journal of Solids and Structures, 44(9) (2007) 2802–2819.
14. Najafizadeh MM, Eslami MR, Thermoelastic stability of circular plates composed of functionally graded materials under uniform radial compression, International Journal of Mechanical Sciences, 44(12) (2002) 2479–93.
15. Navazi HM, Haddadpour H, Rasekh M, An analytical solution for nonlinear cylindrical bending of functionally graded plates, Thin-Walled Structures, 44(11) (2006) 1129–1137.
16. Shariat BAS, Eslami MR. Thermal buckling of imperfect functionally graded plates, International Journal of Solids and Structures, 43(14–15) (2006) 4082–4096.
17. Sundararajan N, Prakash T, Ganapathi M, Influence on functionally graded material on buckling of skew plates under mechanical loads, Finite elements in analysis and design, 42(2) (2005) 152–168.
18. Woo J, Meguid SA, Ong LS, Nonlinear free vibration behaviour of functionally graded plates, Journal of Sound and Vibration, 289(3) (2006) 595–611.
19. Morimoto T, Tanigawa Y, Kawamura R, Thermal buckling analysis of in homogeneous rectangular plate, International Journal of Mechanical Sciences 2006;48(9):926–937.
20. Li SR, Zhang JH, Zhao YG.A theoretical analysis of FGM thin plates, Thin-Walled Structures, 45(5) (2007) 528–536.
21. Wu L. Thermal buckling of a simply supported moderately thick rectangular FGM plate, Composite Structures, 64 (2004):21–28.
22. Chen XL, Liew KM. Buckling of rectangular functionally graded material plates subjected to nonlinearly distributed in-plane edge loads, Smart Materials and Structures, (13) (2004) 1430–7.

23. Yamanouchi M., Koizumi M, Shiota I. in: *Proc. First Int. Symp. Functionally Gradient Materials*, Sendai, Japan (1990) 125-148.
24. Fukui Y, Fundamental investigation of functionally gradient material manufacturing system using centrifugal force. Int. J. Japanese Soci. Mech. Eng. 3 (1991) 144-148.
25.Koizumi M, *FGM Activities in Japan*, Composite*,* 28(1) (1997) 1-4.
26. Praveen GN, Reddy J N, Nonlinear transient thermo elastic analysis of functionally graded ceramic metal plates, International Journal of Solids and Structures, 35 (1998) 4457-4476.
27. Salonitis K, Pandremenos J, Paralikas J, and Chryssolouris G, Multifunctional materials, Engineering applications and Processing Challenges, International Journal of Advanced Manufacturing Technology, 49(5-8)(2008) 803-826.